above arguments, the U value for the pyrazine-bridged complex is larger than that for the triazole-bridged complex. It can be suggested that a direct or through-ligand charge-transfer interaction is important in the propagation of the antiferromagnetic interaction.

It is important to know the molecular orbitals of the bridging ligands in order to predict whether a substantial magnetic interaction exists between the metal centers. MNDO calculations for the organic bridging ligands, which can form dinuclear copper(II) complexes with antiferromagnetic interactions (Table IV), were performed, and the HOMO and related σ orbitals are shown in Figure 4. In the case of the bridging ligands with a negative charge, the energy levels of the pσ orbital, which can coordinate to the copper atoms, are closer in energy to the copper d orbital than that of the bridging ligand without a negative charge. This closer energy difference can cause more mixing of the copper d orbital and nitrogen pσ orbitals, meaning a stronger magnetic interaction in the dinuclear complexes with an anion as the bridging ligand. This character of the molecular orbitals in the bridging ligand is reflected in the magnetic properties; that is, the pyrazine-bridged dinuclear complexes show weaker antiferromagnetic interaction than those with imidazolate and triazolate.

It is also interesting to compare the magnetic interactions of triazole-bridged and triazolato-bridged complexes. The magnetic exchange interactions in dinuclear copper(II) complexes bridged by the triazolate group, $[Cu(bpt)(CF_3SO_3)(H_2O)]_2$ (bpt = 3,5-bis(pyridin-2-yl)-1,2,4-triazolate),[37] and the triazole group, $[Cu(aamt)Br(H_2O)]_2Br_2(H_2O)_2$,[1] are comparable ($J = -102$ to -118 cm^{-1} and $J = -100$ to -110 cm^{-1}, respectively) in spite of the fact that the HOMO and other levels of the triazolate are higher in energy than those of triazole because of the negative charges on the ligand molecule. The stronger antiferromagnetic interaction in the triazolato-bridged complex compared with that in the triazole-bridged one is expected because of the smaller energy difference between copper d and ligand orbitals in the former complex. The conflict of theoretical expectations with the experimental results suggests the importance of geometrical factors of copper and the bridging ligand with respect to the magnetic superexchange interaction.

Acknowledgment. We wish to express our thanks to Dr. Nobuaki Koga (Institute for Molecular Science) for helpful discussions and Dr. Jiro Toyoda (Institute for Molecular Science) for his help in the MNDO calculations.

Supplementary Material Available: Tables listing crystallographic parameters, fractional atomic coordinates for H atoms, anisotropic thermal parameters for non-H atoms, and complete bond lengths and angles, figures showing a packing diagram of the crystal and ESR spectra, and tables of experimental and calculated magnetic susceptibilities (9 pages); a table of structure factors (8 pages). Ordering information is given on any current masthead page.

(38) Anderson, P. W. *Phys. Rev.* **1959**, *115*, 2.
(39) Anderson, P. W. In *Magnetism*; Rado, D. T., Suhl, H., Eds.; Academic Press: New York, 1963; Vol. 1.
(40) Charlot, M. F.; Kahn, O.; Chaillet, M.; Larrieu, C. *J. Am. Chem. Soc.* **1986**, *108*, 2574.

Contribution from the Laboratoire de Chimie Inorganique, URA No. 420, Institut d'Electronique Fondamentale, URA No. 022, Université de Paris-Sud, 91405 Orsay, France, and Groupe de Chimie des Matériaux Inorganiques, EHICS, 1 rue Blaise Pascal, 67008 Strasbourg, France

Magnetism of ACu^{II} Bimetallic Chain Compounds (A = Fe, Co, Ni): One- and Three-Dimensional Behaviors

Petra J. van Koningsbruggen,[1a] Olivier Kahn,*[,1a] Keitaro Nakatani,[1a] Yu Pei,[1a] Jean Pierre Renard,[1b] Marc Drillon,*[,1c] and Patrick Legoll[1c]

Received December 7, 1989

The $ACu(pbaOH)(H_2O)_3 \cdot nH_2O$ chain compounds, hereafter abbreviated as ACu, have been synthesized. A is Fe ($n = 3$), Co, Ni, or Zn ($n = 2$), and pbaOH is 2-hydroxy-1,3-propylenebis(oxamato). These compounds are isomorphous with $MnCu(pbaOH)(H_2O)_3$, of which the crystal structure was known. However, they contain two or three additional water molecules, located between the chains. The magnetic properties have been investigated in the 1.8-300 K temperature range. For A = Fe, Co, and Ni, the $\chi_M T$ versus T plot, χ_M being the molar magnetic susceptibility per ACu unit and T the temperature, shows the minimum characteristic of ferrimagnetic chains. This minimum appears at 95 K for FeCu, 53 K for CoCu, and 80 K for NiCu. At low temperature, the magnetic data are affected by three-dimensional effects. In all the cases, the interchain interactions are antiferromagnetic in nature. CoCu shows a long-range antiferromagnetic ordering at 3.4 K, and NiCu, at 2.9 K. For FeCu, the situation is more complex. The spins of the ferrimagnetic chains do not exactly cancel on the scale of the crystal lattice. There is a canting, which leads to a weak ferromagnetism and a remnant magnetization below the critical temperature $T_c = 10$ K. The magnetic data have been quantitatively interpreted in the temperature range where the three-dimensional effects may be ignored. For NiCu, a ring chain approach has been used, which leads to $J(NiCu) = -81.4$ cm^{-1}; the interaction Hamiltonian is $-J\sum_i S_{A,i}(S_{Cu,i} + S_{Cu,i-1})$. For CoCu and FeCu involving an orbitally degenerate ion A, a model of branch chain has been developed. The interaction between local spins S_A (A = Co, Fe) and S_{Cu} has been assumed to run along the chain axis while the branches have been related to the spin-orbit coupling for Co(II) or Fe(II) ions. In order to solve analytically this problem, it has been further assumed that only z components of spin and orbital momentums were coupled and that the applied field was along the quantization axis. In the frame of this model, the magnetic properties of CoCu and FeCu have been satisfactorily interpreted with $J(CoCu) = -18$ cm^{-1} and $J(FeCu) = -20$ cm^{-1}.

Introduction

A new class of magnetic materials appeared a few years ago, namely the ferrimagnetic chain compounds, in which there is alternation of the magnetic centers A and B along the direction of the chains.[2-6] A and B may be either both metal ions[2-12] or metal ion and organic radical,[13,14] respectively. In other respects, the ferrimagnetic chains may be either regular, the magnetic

(1) (a) Laboratoire de Chimie Inorganique, Université de Paris-Sud. (b) Institut d'Electronique Fondamentale, Université de Paris-Sud. (c) EHICS.
(2) Verdaguer, M.; Julve, M.; Michalowicz, A.; Kahn, O. *Inorg. Chem.* **1983**, *22*, 2624.
(3) Gleizes, A.; Verdaguer, M. *J. Am. Chem. Soc.* **1984**, *106*, 3727.
(4) Beltran, D.; Escriva, E.; Drillon, M. *J. Chem. Soc., Faraday Trans. 2* **1982**, *78*, 1773.
(5) Kahn, O. *Struct. Bonding (Berlin)* **1987**, *68*, 89. Kahn, O. In *Organic and Inorganic Low-Dimensional Crystalline Materials*; Delhaes, P., Drillon, M., Eds.; NATO ASI Series 168; Plenum: New York, 1987; p 93.
(6) Landee, C. P. In *Organic and Inorganic Low-Dimensional Crystalline Materials*; Delhaes, P., Drillon, M., Eds.; NATO ASI Series 168; Plenum: New York, 1987; p 75.
(7) Pei, Y.; Verdaguer, M.; Kahn, O.; Sletten, J.; Renard, J. P. *Inorg. Chem.* **1987**, *26*, 138.

0020-1669/90/1329-3325$02.50/0

centers being then equally spaced, or alternating.[15-18] In the latter case, there is alternation not only of the magnetic centers but also of the exchange pathways as well.

Both one- and three-dimensional properties of the ferrimagnetic chains have been investigated in a thorough manner. In the absence of interchain interaction, the magnetic behavior is quite characteristic. The $\chi_M T$ versus T plot, χ_M being the molar magnetic susceptibility per AB unit and T being the temperature, exhibits a minimum at a finite temperature. When the sample is cooled below this temperature, $\chi_M T$ increases in a ferromagnetic-like fashion and is expected to diverge when T approaches zero. This divergence may be considered as the onset of a long-range magnetic ordering at 0 K. It is indeed well established that there is no magnetic ordering at a finite temperature for a purely one-dimensional system.[19] The spin structure at very low temperature may be schematized as

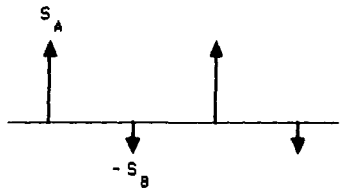

where S_A and S_B ($\neq S_A$) are the local spins, and the system behaves as a chain compound of $|S_A - S_B|$ local spins ferromagnetically coupled. In fact, the chains cannot be perfectly isolated in the crystal lattice. Either they interact between them in an antiferromagnetic fashion, which is the most frequent situation, and the divergence of $\chi_M T$ is stopped at a certain temperature close to the temperature of three-dimensional ordering, or they interact in a ferromagnetic fashion, and below a critical temperature, the system behaves as a ferromagnet. This latter situation was achieved for several Mn(II)–nitronyl nitroxide derivatives[13,14] and $Mn^{II}Cu^{II}$ bimetallic chains.[8,16] One of these chains is the $MnCu(pbaOH)(H_2O)_3$ compound, where pbaOH stands for 2-hydroxy-1,3-propylenebis(oxamato).[8] This compound was obtained through the reaction of Mn(II) ion on the anionic precursor $[Cu(pbaOH)]^{2-}$:

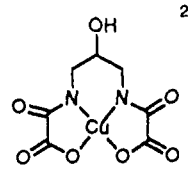

The structure of the chain and of the crystal lattice are recalled in Figure 1. The three-dimensional ferromagnetic ordering was attributed to the fact that, along one of the directions perpendicular to the chain axis, the shortest interchain separations are Mn···Cu instead of Mn···Mn and Cu···Cu.

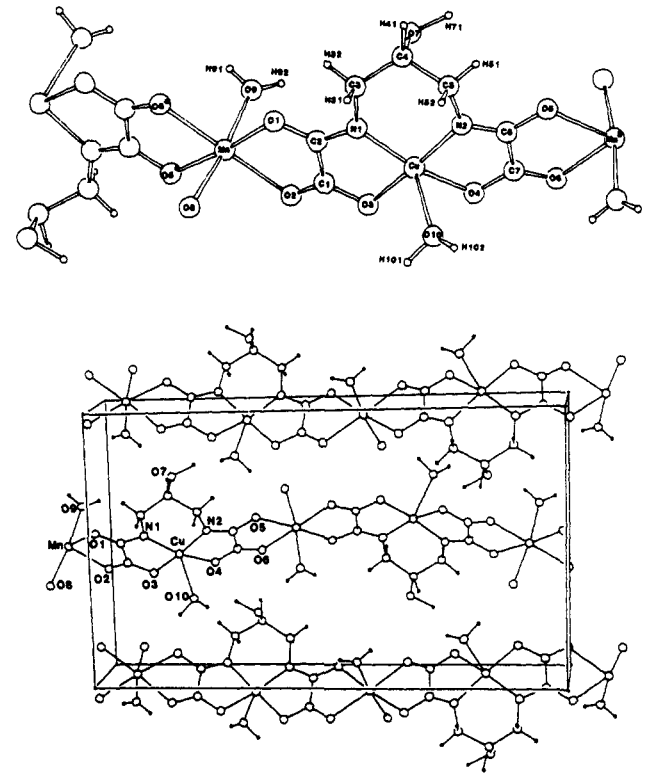

Figure 1. Structure of the chain and of the crystal lattice for $MnCu(pbaOH)(H_2O)_3$.

The paper is devoted to the study of other $A^{II}Cu^{II}$ bimetallic chain compounds prepared from the same $[Cu(pbaOH)]^{2-}$ precursor, A being Fe, Co, Ni, and Zn. Hereafter, the compounds are abbreviated as ACu. In this work, we pursue a double goal, first to study qualitatively and quantitatively the one-dimensional magnetic behavior of the compounds and then to determine the nature of the three-dimensional ordering.

Concerning the former goal, we will focus on the FeCu and CoCu compounds in which the A(II) ion is orbitally degenerate. To interpret quantitatively the magnetic properties, we will develop a model where the ACu bimetallic chain is treated as a branch chain with two kinds of interactions: one between local spins S_A and S_{Cu} along the chain, the other one between S_A and the local angular momentum L_A along each branch. This model, for which the status will be discussed, will be also utilized for interpreting the magnetic properties of the $ANi(pbo)\cdot nH_2O$ chain compounds (abbreviated as ANi) in which the A(II) ions may be considered to be magnetically isolated. Indeed, the Ni(II) ion in planar surroundings is diamagnetic, and the M···M shortest separation along the chain is on the order of 11 Å. $ANi(pbo)\cdot nH_2O$ is obtained through the reaction of A(II) on the diamagnetic precursor $[Ni(pbo)]^{2-}$, with pbo = 1,3-propylenebis(oxamido):

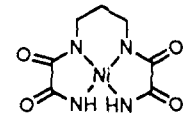

Experimental Section

Syntheses. The synthesis of the compounds $ACu(pbaOH)(H_2O)_3\cdot 2H_2O$, with A = Co, Ni, and Zn, was carried out from the reaction of A(II) on $Na_2[Cu(pbaOH)]\cdot 4.5H_2O$, according to the method described for the manganese derivative.[8] Anal. Calcd for $C_7H_{16}N_2O_{12}CuCo$: C, 19.70; H, 3.75; N, 6.57; Cu, 14.89; Co, 13.81. Found: C, 19.92; H, 3.86; N, 6.60; Cu, 14.15; Co, 13.14. Calcd for $C_7H_{16}N_2O_{12}CuNi$: C, 19.17; H, 3.62; N, 6.39; Cu, 14.36; Ni, 13.31. Found: C, 19.30; H, 3.40; N, 6.18; Cu, 14.12; Ni, 12.86. Calcd for $C_7H_{16}N_2O_{12}CuZn$: C, 18.71; H, 3.56; N, 6.24; Cu, 14.14; Co, 14.57. Found: C, 18.54; H, 3.43; N, 6.00; Cu, 14.11; Co, 14.33.

(8) Kahn, O.; Pei, Y.; Verdaguer, M.; Renard, J. P.; Sletten, J. *J. Am. Chem. Soc.* **1988**, *110*, 782.
(9) Drillon, M.; Gianduzzo, J. C.; Georges, R. *Phys. Lett.* **1983**, *96A*, 413.
(10) Drillon, M.; Coronado, E.; Beltran, D.; Curely, J.; Georges, R.; Nugteren, P. R.; De Jongh, L. J.; Genicon, J. L. *J. Magn. Magn. Mater.* **1986**, *54–57*, 1507.
(11) Coronado, E.; Drillon, M.; Nugteren, P. R.; de Jongh, L. J.; Beltran, D. *J. Am. Chem. Soc.* **1988**, *110*, 3907.
(12) Coronado, E.; Drillon, M.; Nugteren, P. R.; de Jongh, L. J.; Beltran, D.; Georges, R. *J. Am. Chem. Soc.* **1989**, *111*, 3874.
(13) Caneschi, A.; Gatteschi, D.; Rey, P.; Sessoli, R. *Inorg. Chem.* **1988**, *27*, 1756.
(14) Caneschi, A.; Gatteschi, D.; Renard, J. P.; Rey, P.; Sessoli, R. *Inorg. Chem.* **1989**, *28*, 1976. *Ibid.* **1989**, *28*, 2940.
(15) Pei, Y.; Kahn, O.; Sletten, J.; Renard, J. P.; Georges, R.; Gianduzzo; Curely, J.; Xu, Q. *Inorg. Chem.* **1988**, *27*, 47.
(16) Nakatani, K.; Carriat, J. Y.; Journaux, Y.; Kahn, O.; Lloret, F.; Renard, J. P.; Pei, Y.; Sletten, J.; Verdaguer, M. *J. Am. Chem. Soc.* **1989**, *111*, 5739.
(17) Pei, Y.; Nakatani, K.; Kahn, O.; Sletten, J.; Renard, J. P. *Inorg. Chem.* **1989**, *28*, 3170.
(18) Georges, R.; Curely, J.; Gianduzzo, J. C.; Quiang, X.; Kahn, O.; Pei, Y. *Physica* **1988**, *B153*, 77.
(19) Carlin, R. L. *Magnetochemistry*, Springer-Verlag, Berlin, 1986.

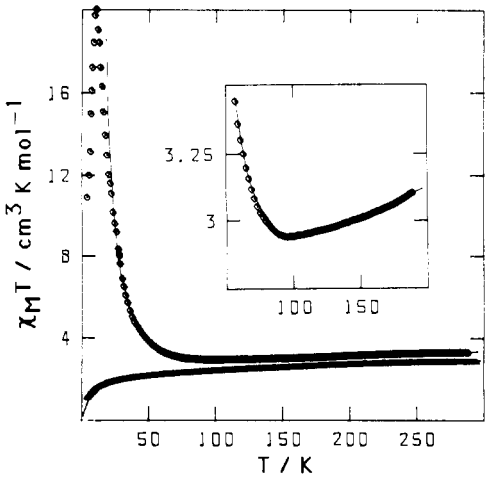

Figure 2. Experimental $\chi_M T$ versus T plot for FeCu (O) and FeNi (Δ) and calculated curves (—).

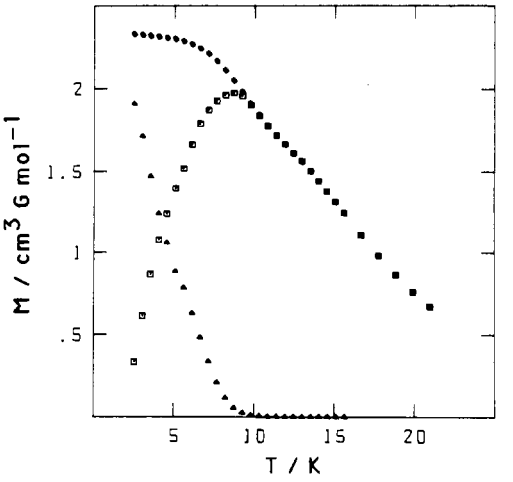

Figure 3. Temperature dependence of the magnetization for FeCu within a magnetic field of 1 G: (O) FCM; (Δ) remnant magnetization; (□) ZFCM.

The synthesis of $FeCu(pbaOH)(H_2O)_3 \cdot 2H_2O$ was carried out as follows: A solution containing 10^{-3} mol of $Na_2[Cu(pbaOH)] \cdot 4.5H_2O$ in 15 mL of water was added to a solution containing 1.3×10^{-3} mol of $FeSO_4 \cdot (NH_4)_2SO_4 \cdot 6H_2O$ in 15 mL of water. $FeCu(pbaOH)(H_2O)_3 \cdot 3H_2O$ precipitated as a green polycrystalline powder. Anal. Calcd for $C_7H_{18}N_2O_{13}CuFe$: C, 18.37; H, 3.94; N, 6.12; Cu, 15.20; Fe, 12.18. Found: C, 18.82; H, 3.64; N, 6.17; Cu, 14.69; Fe, 12.20.

The compounds $ANi(pbo)(H_2O)_2 \cdot xH_2O$, with A = Fe, and $x = 4$ and A = Co and $x = 4.5$, were synthesized as follows. An aqueous solution of $Na_2[Ni(pbo)] \cdot 4.5H_2O$ prepared as described by Nonoyama et al.[20] was added to an aqueous solution of $A^{II}(ClO_4)_2$. $ANi(pbo)(H_2O)_2 \cdot 4H_2O$ precipitated as a microcrystalline powder. Anal. Calcd for $C_7H_{22}N_4O_{10}NiFe$: C, 18.65; H, 4.44; N, 12.43; Ni, 13.02; Fe, 12.39. Found: C, 18.68; H, 4.31; N, 12.80; Ni, 12.51; Fe, 12.76. Calcd for $C_7H_{23}N_4O_{10.5}NiCo$: C, 18.56; H, 4.42; N, 12.37; Ni, 12.97; Co, 13.01. Found: C, 18.96; H, 3.95; N, 12.42; Ni, 12.88; Co, 12.93.

Magnetic Measurements. These were carried out with a Faraday-type magnetometer equipped with a helium continuous-flow cryostat in the 4.2–300 K temperature range and with a laboratory-made low-field SQUID magnetometer in the 1.8–20 K temperature range. $HgCo(NCS)_4$ was used as a susceptibility standard. Diamagnetic corrections were taken as -140×10^{-6} cm^3 mol^{-1} for ACu (A = Co, Ni, Zn), -150×10^{-6} cm^3 mol^{-1} for FeCu, -160×10^{-6} cm^3 mol^{-1} for FeNi, and -165×10^{-6} cm^3 mol^{-1} for CoNi.

EPR Spectra. The X-band powder spectra were recorded with a ER 200D Bruker spectrometer equipped with a helium continuous-flow cryostat, a Hall probe, and a frequency meter.

Magnetic Properties: Qualitative Approach

FeCu. The $\chi_M T$ versus T plot is shown in Figure 2, χ_M being the molar magnetic susceptibility per FeCu unit and T being the temperature. $\chi_M T$ is equal to 3.30 cm^3 K mol^{-1} at room temperature, smoothly decreases upon cooling and reaches a minimum around 95 K with $\chi_M T = 2.94$ cm^3 K mol^{-1}. This rounded minimum of $\chi_M T$ is the signature of the one-dimensional ferrimagnetic behavior. When the sample is cooled further, $\chi_M T$ increases more and more rapidly and then reaches a sharp maximum around 10 K with a $\chi_M T$ value as large as 20 cm^3 K mol^{-1}. Below 10 K, $\chi_M T$ falls down. This sharp maximum of $\chi_M T$ suggests that the $Fe^{II}Cu^{II}$ ferrimagnetic chains tend to order antiferromagnetically on the scale of the crystal lattice.

To get more information about the three-dimensional magnetic behavior of the compound, we investigated the temperature dependence of the molar magnetization M in the temperature range $2 < T/K < 20$. The results are shown in Figure 3. The field-cooled magnetization (FCM) is obtained by cooling within a magnetic field of 1 G. This FCM increases when the sample is cooled and then below 7 K tends to a plateau with a M value of roughly 2.3 cm^3 G mol^{-1}. This plateau might be due to demagnetization effects. When the field is switched off at 2 K, a remnant magnetization is detected, which vanishes above T_c = 10 K. The zero-field-cooled magnetization (ZFCM) is obtained by cooling in zero field and then warming within the field of 1 G. At any temperature below T_c, the ZFCM is smaller than the FCM due to the fact that the temperature is too low in order for the ferromagnetic domain walls to move freely. The ZFCM curve exhibits a maximum at T_c, as expected for a ferromagnetic powder sample.[21] The fact that the compound exhibits a zero-field magnetization is not in contradiction with the antiferromagnetic nature of the interchain couplings. The magnetization at 3 K induced with a field of 1 G remains quite weak. For $MnCu(pbaOH)(H_2O)_3$, the magnetization induced with the same field, at the same temperature, was equal to 500 cm^3 G mol^{-1}, i.e. 2 orders of magnitude stronger.[7] Actually, the magnetization observed in FeCu is typical of a weak ferromagnetism. Within the crystal lattice, the spins of adjacent ferrimagnetic chains tend to compensate each other, with however a small canting so that the resulting spin is not exactly zero.

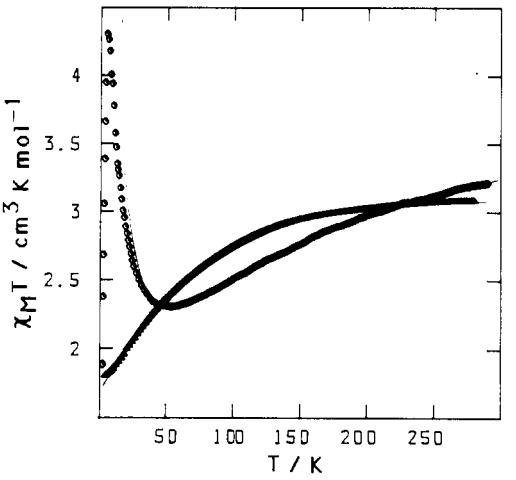

Figure 4. Experimental $\chi_M T$ versus T plot for CoCu (O) and CoNi (Δ) and calculated curves (—).

CoCu. The $\chi_M T$ versus T plot shown in Figure 4 exhibits all the features of ferrimagnetic chains with antiferromagnetic interchain couplings. $\chi_M T$ is equal to 3.21 cm^3 K mol^{-1} at room temperature. The rounded minimum is observed about 53 K with $\chi_M T = 2.31$ cm^3 K mol^{-1} and the sharp maximum at 5 K with $\chi_M T = 4.31$ cm^3 K mol^{-1}. The maximum of χ_M corresponding to the onset of the three-dimensional antiferromagnetic ordering is observed at $T_N = 3.4$ K (see Figure 5). The magnetization study does not reveal any weak ferromagnetism.

(20) Nonoyama, K.; Ojima, H.; Nonoyama, M. *Inorg. Chim. Acta* **1976**, *20*, 127.

(21) Hitzfeld, M.; Ziemann, P.; Buckel, W.; Claus, H. *Phys. Rev. B* **1984**, *29*, 5023.

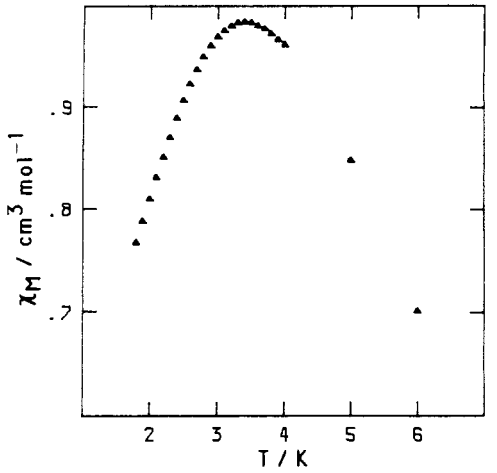

Figure 5. χ_M versus T plot for CoCu in the 1.8–6 K temperature range.

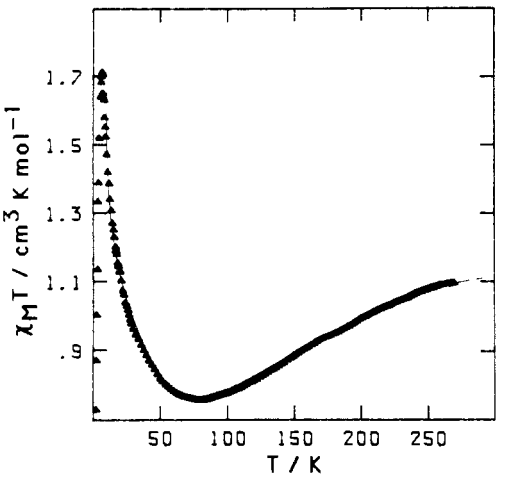

Figure 6. Experimental $\chi_M T$ versus T plot for NiCu (△) and calculated curve (—).

NiCu. The magnetic behavior represented in Figure 6 is again characteristic of ferrimagnetic chains with antiferromagnetic interchain interaction. $\chi_M T$ is equal to 1.10 cm^3 K mol^{-1} at 270 K, decreases upon cooling, reaches a minimum around 80 K with $\chi_M T$ = 0.76 cm^3 K mol^{-1}, increases upon cooling further, and finally shows a maximum at 7 K. The maximum of χ_M due to the onset of a three-dimensional antiferromagnetic ordering appears at T_N = 2.9 K.

ZnCu. The magnetic behavior is essentially that of isolated copper(II) ions. $\chi_M T$ is constant in the 300–10 K temperature range and is equal to 0.39 cm^3 K mol^{-1}. When the sample is cooled below ca. 10 K, $\chi_M T$ weakly decreases and reaches a value of 0.30 cm^3 K mol^{-1} at 1.2 K.

FeNi and CoNi. In both cases, $\chi_M T$ decreases when T is lowered, which corresponds to well-known behavior for Fe(II) and Co(II) isolated ions.[19] This is due to the fact that spin–orbit coupling and local distortion split the orbitally degenerate ground terms and lead to several thermally populated low-lying states at room temperature. The limits values are $\chi_M T$ = 2.84 cm^3 K mol^{-1} at 294 K and 1.08 cm^3 K mol^{-1} at 4.2 K for FeNi and $\chi_M T$ = 3.08 cm^3 K mol^{-1} at 280 K and 1.80 cm^3 K mol^{-1} at 4.2 K for CoNi. The $\chi_M T$ versus T plots for FeNi and FeCu are both displayed in Figure 2, and those for both CoNi and CoCu, in Figure 4. This shows in a spectacular fashion the polarization effect of the Cu(II) ions in the ferrimagnetic chains and the ferromagnetic-like behavior below the temperature of the minimum of $\chi_M T$.

EPR Spectra. They have been recorded on powder samples. All the ACu compounds studied in this paper are EPR silent at any temperature in the range 4.2–300 K, with the exception of ZnCu, for which the spectrum is typical of tetragonally elongated isolated copper(II) ion with $g_\parallel$ = 2.23 and $g_\perp$ = 2.07. The reasons why FeCu and NiCu are EPR silent actually remain unclear for us, and we would like to focus on this problem in the near future.

Magnetic Properties: Quantitative Approach

FeCu and CoCu. To describe the one-dimensional magnetic behavior of these compounds, we introduce a new model, namely the "branch chain model". The magnetic system of interest is represented by the branch chain

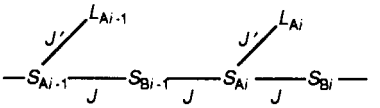

The interaction is assumed to run along the z chain axis, while the branches are related to the spin–orbit coupling for the orbitally degenerate ion Fe(II) or Co(II). This scheme does not describe the actual topology of the chains, but indicates the relevant topology occurring when half of the magnetic centers are orbitally degenerate. In this respect, the FeCu or CoCu elementary unit is described by a S_A–L_A–S_B scheme, L_A standing for the orbital momentum of Fe(II) or Co(II), so that the overall multiplicity of the problem is 15 × 2/FeCu unit, and 12 × 2/CoCu unit. The Hamiltonian for such a branch chain may be written as

$$\mathcal{H} = \sum_i \{-J[S_{A,i(z)}\cdot(S_{B,i(z)} + S_{B,i-1(z)})] + J' L_{A,i(z)}\cdot S_{A,i(z)} + D L_{A,i(z)}^2 - \beta H(g_A S_{A,i(z)} + g_B S_{B,i(z)} + k L_{A,i(z)})\} \quad (1)$$

where i runs over AB units, A referring to Fe(II) or Co(II) and B to Cu(II). The index (z) notes the z component of the spin or angular momentum. J and J' are the interaction and spin–orbit coupling parameters, respectively. D is the local anisotropy parameter for the A ion, and k is a covalency factor. The expression of the local spin–orbit coupling in (1) is obviously not rigorously correct, but is justified by the necessity to have an anisotropic operator to use the transfer matrix technique. Actually, owing to the competition between spin–orbit coupling and local distortion for the orbitally degenerate ion A, it can be shown that the fictious Hamiltonian (1) involving only $L_{A,(z)}$ and $S_{A,(z)}$ components of the orbital and spin operators describes quite well the real system. However, the significance of the effective parameters J' and D differs from that of the genuine spin–orbit coupling and distortion parameters, J' and D correspond to a mixing of these genuine parameters. One may also notice that numerical computations on finite chains on increasing size would be intractable in the present case due to the spin and orbital degeneracies of the interacting ions.

Let us consider first the CoCu compound. The relevant quantum numbers are $S_A = {}^3/_2$, $L_A = 1$, and $S_B = {}^1/_2$. The eigenvalues of (1) can be derived exactly by using the transfer-matrix technique since only z components of the spin and angular momentums are considered and the external field is assumed to be applied along the quantization axis. This approximation can be justified by the nature of the Co(II) ion, which forces the interaction to be highly anisotropic.[11] In the limit of very long chains, all the thermodynamical functions of interest may be derived from the expression of the transfer operator **T**, linking the partition functions when adding an extra CoCu unit. **T** may be expressed as

$$\mathbf{T} = \mathbf{T}_1 \otimes \mathbf{T}_2 \quad (2)$$

where $\mathbf{T}_1$ deals with the 2 × 12 matrix from Cu(II) to Co(II) and $\mathbf{T}_2$ with the 12 × 2 matrix from Co(II) to Cu(II). The terms of $\mathbf{T}_1$ and $\mathbf{T}_2$ are derived from the Hamiltonian (1) as

$$a_{pq} = \langle \varphi_{A,p}\varphi_{B,q}|e^{-\beta H}|\varphi_{A,p}\varphi_{B,q}\rangle$$
$$b_{pq} = \langle \varphi_{B,p}\varphi_{A,q}|e^{-\beta H}|\varphi_{B,p}\varphi_{A,q}\rangle \quad (3)$$

where φ_A and φ_B refer to $(S_{A,(z)}, L_{A,(z)})$ and $S_{B,(z)}$, respectively. Accordingly, the matrix **T** for the overall CoCu chain reduces to a 2 × 2 or 12 × 12 matrix, depending on the product $\mathbf{T}_1 \otimes \mathbf{T}_2$ or $\mathbf{T}_2 \otimes \mathbf{T}_1$ under consideration. The **T**, $\mathbf{T}_1$, and $\mathbf{T}_2$ matrices are given as supplementary material. It can be shown that the largest

eigenvalue is identical for both products and is nothing but the partition function per CoCu unit. For a nonvanishing magnetic field H, this quantity can be expressed as a power series of H, as

$$E_+(H) = E_+(0) + \alpha H^2 + \dots \quad (4)$$

with, in the present case

$$E_+(0) = 8e^z(\cosh^2 3x \cosh 3y + \cosh^2 x \cosh y) + 4(\cosh^2 x \cosh^2 3x) \quad (5)$$

x, y, and z being defined as

$$x = J/4kT$$
$$y = -J'/2kT$$
$$z = -D/kT \quad (6)$$

The absence of the linear term in H in (4) is due to the fact that the magnetization defined as $-\partial E_+(H)/\partial H$ vanishes in zero-field. The magnetic susceptibility is then readily calculated from the second derivative of ln $[E_+(H)]$ with respect to H, namely

$$\chi_M = [NkT/E_+(0)][\partial^2 E_+(H)/\partial H^2]$$

The zero-field susceptibility is given by

$$\chi_M = (N\beta^2/kT)[u^2a + 2uc + (ua + c)^2/b + d]/(a + b) \quad (7)$$

with

$$a = (2e^z \cosh 3y + 1) \cosh 6x + (2e^z \cosh y + 1) \cosh 2x$$

$$b = 2[e^z(\cosh 3y + \cosh y) + 1]$$

$$c = \{e^z[e^{-3y}(3v - k) + e^{3y}(3v + k)] + 3v\} \sinh 6x + [e^z(e^{-y}(v - k)) + e^y(v + k) + v] \sinh 2x$$

$$d = \{e^z[e^{-3y}(3v - k)^2 + e^{3y}(3v + k)^2] + (3v)^2\}(1 + \cosh 6x) + \{e^z[e^{-y}(v - k)^2 + e^y(v + k)^2] + v^2\}(1 + \cosh 2x) \quad (8)$$

and

$$u = g_B/2$$
$$v = g_A/2 \quad (9)$$

For $|J'| \gg |J|$, the spin–orbit coupling is the leading effect, stabilizing a local Kramers doublet for the Co(II) ion. The expression of χ_M then reduces in the low-temperature limit ($kT \ll |J'|$) to that reported for the CoCu(edta)·$6H_2O$ compound in which the Co–Cu interaction is very small.[11] This limit expression is

$$\chi_M = (N\beta^2/2kT)[g_+^2 \exp(J/2kT) + g_-^2 \exp(-J/2kT)] \quad (10)$$

with

$$g_\pm = (g_A \pm g_B)/2 \quad (11)$$

Let us first discuss the temperature dependence of $\chi_M T$ for various combinations of J, J', and D parameters, the other parameters remaining constant, with $g_A = g_B = 2$ and $k = 1$. Figure 7 deals with $J' > 0$ and Figure 8 with $J' < 0$. In all cases, $|D/J'|$ is equal to 2.5. For $J < 0$, $\chi_M T$ exhibits a minimum at a temperature on the order of $|J|/k$ and then a swift increase at lower temperature. The minimum of $\chi_M T$ is more pronounced for $D < 0$ than for $D > 0$. When J/J' is zero, the local spins $S_A = {}^3/_2$ feel no exchange field and behave as if they were free. $\chi_M T$ is then the sum of a temperature-independent term due to Cu(II) ions and a temperature-dependent one reflecting the spin–orbit coupling on the Co(II) ions. Finally, when J is positive and large enough, $\chi_M T$ regularly increases upon cooling down, whatever the sign of D may be. It is likely worth mentioning that a minimum of $\chi_M T$ may also be obtained for positive and very small values of J/J'. This results from the occurrence of two regimes in the magnetic behavior. For temperatures higher than J'/k, $\chi_M T$ decreases upon cooling down in relation with the influence of the spin–orbit coupling for orbitally degenerate sites. In turn, at lower temperature, the ferromagnetic interaction between nearest neighbors

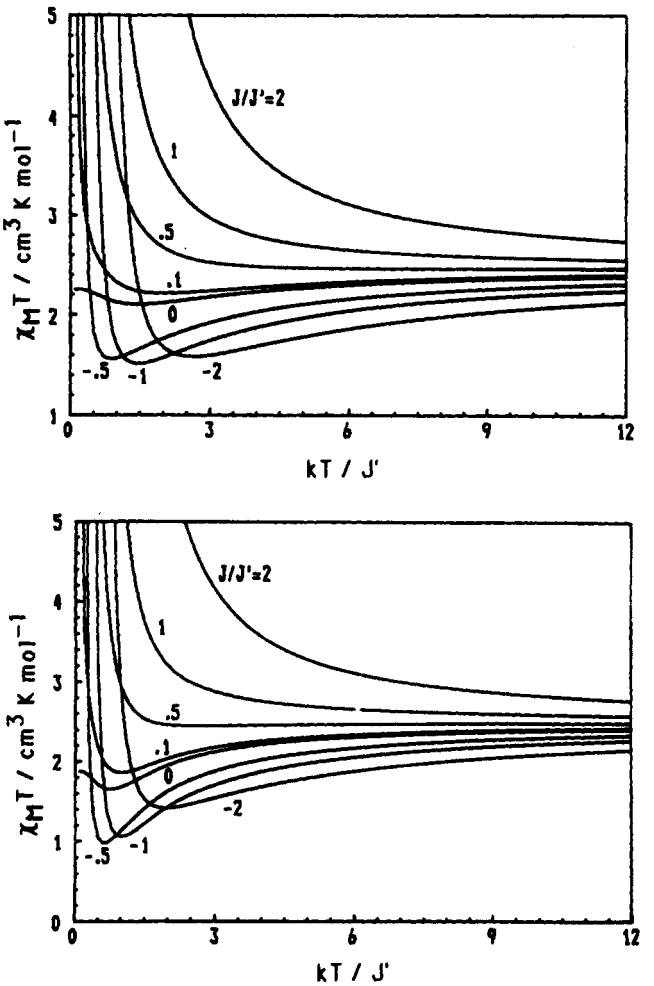

Figure 7. Theoretical variations of $\chi_M T$ versus T for a CoCu chain, with $J' > 0$, $g_A = g_B = 2$, $k = 1$, and various J/J' ratios: top, $D/J' = +2.5$; bottom, $D/J' = -2.5$.

entails a strong divergence of $\chi_M T$. It follows that in this very peculiar situation, the behavior may be ferrimagnetic-like although the interaction is ferromagnetic! To finish with this discussion, it is important to recall that only the parallel component of the magnetic susceptibility is considered; it has already been pointed out that the perpendicular component is weak and very slightly temperature dependent in the temperature range of interest, so that it can be treated as a constant term.[11]

The least-squares fitting of the experimental data with our model was limited to the temperature range where the three-dimensional effects can be ignored, namely in the 30–300 K range. It led to a fairly good theory–experiment agreement (see Figure 4) with $J = -18$ cm^{-1}, the other parameters being $J' = -31$ cm^{-1}, $D = 114$ cm^{-1}, $g_{Co} = 2.32$, and $g_{Cu} = 2.02$.

The same approach may be used for the FeCu compound with $S_A = 2$ and $L_A = 1$. Equation 4 remains valid, the a–d terms being now expressed as

$$a = (2e^z \cosh 2y + 1) \cosh 4x + (2e^z \cosh y + 1) \cosh 2x + e^z + {}^1/_2$$

$$b = e^z(2 \cosh 2y + 2 \cosh y + 1) + {}^5/_2$$

$$c = \{e^z[e^{2y}(2g_A - k) + e^{-2y}(2g_A + k)] + 2g_A\} \sinh 4x + \{e^z[e^y(g_A - k) + e^{-y}(g_A + k)] + g_A\} \sinh 2x$$

$$d = \{e^z[e^y(2g_A - k)^2 + e^{-2y}(2g_A + k)^2] + (2g_A)^2\}(1 + \cosh 4x) + \{e^z[e^y(g_A - k)^2 + e^{-y}(g_A + k)^2] + g_A^2\}(1 + \cosh 2x) + 2e^z k^2 \quad (12)$$

with

$$x = J/kT \quad (13)$$

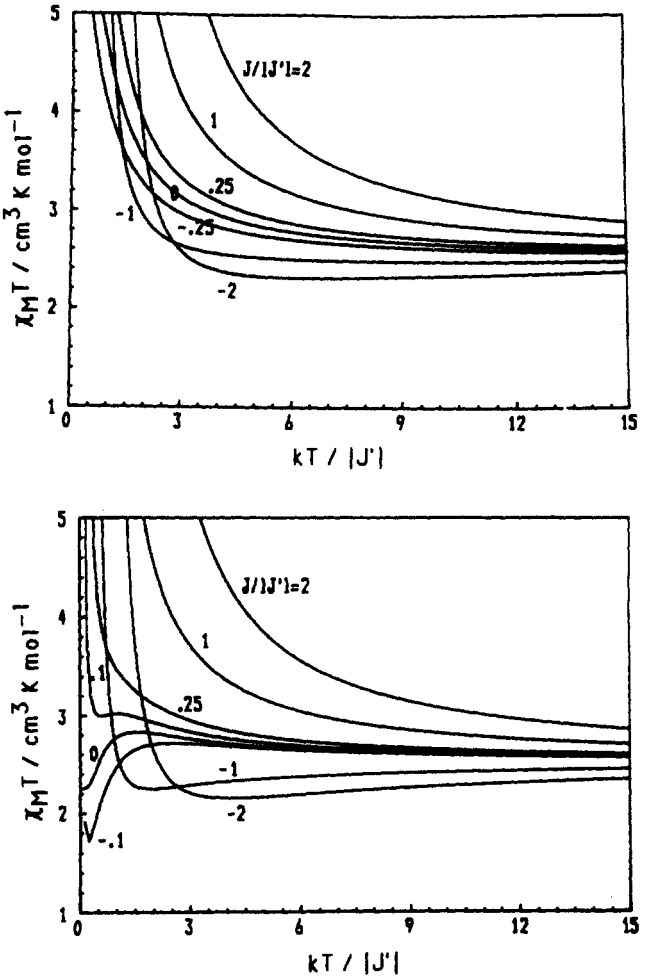

Figure 8. Theoretical variations of $\chi_M T$ versus T for a CoCu chain, with $J' < 0$, $g_A = g_B = 2$, $k = 1$, and various J/J' ratios: top, $D/J' = -2.5$; bottom, $D/J' = +2.5$.

u, v, y, and z being defined as in (6).

The least-squares fitting of the experimental $\chi_M T$ values above 30 K led to $J = -20$ cm^{-1}, with $J' = -73$ cm^{-1}, $D = -7$ cm^{-1}, $g_{Fe} = 2.0$, and $g_{Cu} = 2.17$ (see Figure 2).

We also attempted to fit the experimental data for CoCu and FeCu with the recently proposed classical–quantum model,[15,18] S_{Co} or S_{Fe} being treated as a classical spin and S_{Cu} as a quantum spin. The only parameters are then J, g_A, and g_B. This model leads to a less satisfactory theory–experiment agreement. The agreement factor defined as $\Sigma[(\chi_M T)^{obs} - (\chi_M T)^{cal}]^2/[(\chi_M T)^{obs}]^2$ is 1 order of magnitude higher. However, the J values are not much different. They are found as −23 cm^{-1} for CoCu and −25 cm^{-1} for FeCu.

CoNi and FeNi. The model presented above can be utilized for interpreting quantitatively the magnetic properties for CoNi and FeNi. In this case, only the orbital degeneracy of Co(II) or Fe(II) contributes to the $\chi_M T$ variation. An excellent theory–experiment agreement was obtained with $J' = 21$ cm^{-1}, $D = 15$ cm^{-1}, and $g_{Co} = 2.45$ for CoNi and $J' = 35$ cm^{-1}, $D = 42$ cm^{-1}, and $g_{Fe} = 2.00$ for FeNi (see Figures 4 and 2). It can be noticed that the fitting is not very sensitive to D, so that the uncertainty on this parameter may be rather large.

One will notice that the single-ion parameters J', D, and g_A are not transferable from ANi to ACu, which is not quite surprising since the bridging ligands are not rigorously the same in the two series.

NiCu. The magnetic susceptibility of an AB alternating chain with $S_A = 1$ and $S_B = {}^1/_2$ has been calculated by using the ring chain technique and in the approximation where the g_A and g_B factors are assumed to be equal ($g_A = g_B = g$), the result has been fitted with the analytical expression[24]

$$\chi_M T = (N\beta^2 g^2/k)(ax^3 + bx^2 + cx + d)/(ex^2 + fx + d) \quad (14)$$

with

$$a = -0.034\,147$$
$$b = 2.8169$$
$$c = -7.2320$$
$$d = 11$$
$$e = 1.2966$$
$$f = 0.697\,19$$
$$g = 12 \quad (15)$$

and

$$x = |J|/kT \quad (16)$$

Equation 14 is only valid for $J < 0$. The least-squares fitting of the experimental data with eq 11 in the temperature range 20–290 K where the three-dimensional effects are not perceptible yet leads to $J = -81.4$ cm^{-1} and $g = 2.15$ (see Figure 6). Those results are identical within the experimental uncertainties to those obtained for $NiCu(pba)(H_2O)_3 \cdot 2H_2O$.[7]

Discussion and Conclusion

The first point we wish to discuss concerns the crystal structure of the $ACu(pbaOH)(H_2O)_3 \cdot nH_2O$ chain compounds. Only the A = Mn derivative has been obtained in the form of single crystals suitable for X-ray study, and its structure is recalled in Figure 1. According to the powder X-ray patterns, all the other compounds with A = Fe, Co, Ni, and Zn are strictly isomorphous with the manganese derivative. However, the chemical analyses indicate that they contain either two (A = Co, Ni, Zn) or three (A = Fe) additional water molecules. Therefore, these compounds may be structurally described as regular bimetallic chains running along the b axis of the orthorhombic lattice. The shortest interchain separations are A···Cu along the a direction, and A···A and Cu···Cu along the c direction. In addition to the two water molecules linked to each manganese atom and the water molecule linked to each copper atom, there are two (or three for FeCu) noncoordinated water molecules between the chains. It can be mentioned here that the compound $MnCu(pba)(H_2O)_3 \cdot 2H_2O$ of which the structure has been described also contains two noncoordinated water molecules.[7]

One of the goals of this work was to see whether the long-range ferromagnetic ordering observed in $MnCu(pbaOH)(H_2O)_3$ would be retained when replacing the Mn(II) ions with $^5/_2$ local spins by other ions with smaller local spins. The answer is no. For all the bimetallic chains investigated in this paper, the interchain interactions are antiferromagnetic in nature, so that the spins of the ferrimagnetic chains tend to cancel on the scale of the crystal lattice. In the case of FeCu, however, there is a spin canting, which leads to a weak ferromagnetism and a remnant magnetization below the critical temperature $T_c = 10$ K. This work confirms that the mechanism of the ferromagnetic ordering observed in some $Mn^{II}Cu^{II}$ chains as well as in some Mn(II)–nitronyl nitroxide compounds is complex. In the ACu chains, there is apparently a subtle balance between antiferro- and ferromagnetic contributions, this latter being the more pronounced when the S_A spin is the larger. If so, this would substantiate the role of the dipolar interactions in the ferromagnetic ordering.[13,14,22,23]

It is worth noting that CoCu also exhibits a three-dimensional antiferromagnetic ordering with $T_N = 3.4$ K. Another $Co^{II}Cu^{II}$ chain compound has been reported, namely $CoCu(edta)(H_2O)_4 \cdot 2H_2O$ with edta = ethylenediaminetetraacetato.[11] This compound shows no long-range ordering, which has been

(22) Gatteschi, D.; Guillou, O.; Zanchini, C.; Sessoli, R.; Kahn, O.; Verdaguer, M.; Pei, Y. *Inorg. Chem.* **1989**, *28*, 287.
(23) Gatteschi, D.; Zanchini, C.; Kahn, O.; Pei, Y. *Chem. Phys. Lett.* **1989**, *160*, 157.
(24) Drillon, M.; Coronado, E.; Georges, R.; Gianduzzo, J. C.; Curely, J. *Phys. Rev.* **1989**, *40*, 10992.

attributed to the fact that in the AB(edta) family the long-range ordering, if any, occurs at very low temperature, below 1 K. In this temperature range, only the ground Kramers doublet for Co(II) is thermally populated, and the Co(II)–Cu(II) intrachain interaction involving effective spins $^1/_2$ leads to a nonmagnetic ground state. In our case, both intra- and interchain interactions are much more pronounced, so that it is no longer possible to ignore the population of local excited states for Co(II). In other terms, treating Co(II) as an effective spin $^1/_2$ is no longer a good approximation.

To take into account the orbital degeneracy of cobalt(II) and iron(II), we have introduced a branch chain model with z–z interactions between nearest-neighbor local spins S_A and S_B along the chain, and an anisotropic coupling between local spin S_A and local angular momentum L_A along each branch. The intrinsic limit of this model arises from the fact that the magnetic field is assumed to be applied along the z quantization axis; otherwise, the derivation of the thermal properties would not be feasible. This model allows us to reproduce fairly well the magnetic properties of the CoCu and FeCu compounds in the temperature range where the three-dimensional effects may be ignored. Our model has also been tested in the simple case where S_B is zero, B being Ni(II) in a square-planar environment. The rather large values of the intrachain interaction parameters in ACu chain compounds with A = Mn, Fe, Co, and Cu confirm, if it was still necessary, the remarkable ability of conjugated bisbidentate bridging ligands like oxamato to transmit the electronic effects between magnetic centers far apart from each other. The A···Cu separation through the oxamato bridge is indeed about 5.4 Å.

Since the branch chain model is novel, at least in the context of the ferrimagnetic chains, it seems to us interesting to sum up briefly the various models proposed so far to interpret the magnetic properties of ferrimagnetic chains.

(i) Chronologically, the first model is that of $(AB)_N$ ring chains of increasing size, the local spins S_A and S_B being explicitely treated as quantum spins.[2,9,24] The only limitation of this model is the storage capacity of the available computers.

(ii) When both S_A and S_B are large enough, they can be treated as classical spins. An approach of this kind has been developed. This approach leads to an analytical expression for the magnetic susceptibility.[25]

(iii) A classical–quantum model has also been proposed.[26,27] This model, valid when one of the two local spins is large and the other one small, has been applied to the Mn(II)Cu(II) chains.[3,7,8] It has recently been extended to the case of the alternating bimetallic chains.[15,18]

(iv) The anisotropic Ising-type chain has also been investigated for S_A ranging from $^1/_2$ to infinite, S_B remaining equal to $^1/_2$.[28,29] One of the striking results is the occurrence of a compensation temperature, similar to that of three-dimensional ferrimagnets, for a critical ratio between local magnetic momentums g_AS_A and g_BS_B.

(v) The models mentioned above are not valid a priori when at least one of the magnetic centers, e.g., A, is orbitally degenerate. If the orbital degeneracy leads to a ground Kramers doublet, the actual spin S_A of the orbitally degenerate ion may be replaced by an effective spin $^1/_2$. Such an approximation is restricted to the case where the interaction parameter is very small with respect to the energy gap between the ground Kramers doublet and the first excited state. The intrachain interaction may then be considered as of the Ising-type, and model iv becomes relevant.

(vi) Finally, the model developed in this paper is valid for any situation of orbital degeneracy, whatever the magnitude of the intrachain interaction.

To finish with, it is worth mentioning that the application of the branch chain model to the case of bimetallic chains involving an orbital degeneracy is an extension of a work carried by one of us on exotic magnetic systems.[30,31]

Acknowledgment. We express our deepest gratitude to the Société Nationale Elf Aquitaine, which has financially supported this work and offered a research grant to K.N.

Supplementary Material Available: A table of the T, T_1, and T_2 matrices for the CoCu chain compound (3 pages). Ordering information is given on any current masthead page.

(25) Drillon, M.; Coronado, E.; Beltran, D.; Georges, R. *Chem. Phys.* **1983**, *79*, 449.

(26) Seiden, J. *J. Phys., Lett.* **1983**, *44*, L947.

(27) Verdaguer, M.; Gleizes, A.; Renard, J. P.; Seiden, J. *Phys. Rev.* **1984**, *B29*, 5144.

(28) Curely, J.; Georges, R.; Drillon, M. *Phys. Rev.* **1986**, *B33*, 6243.

(29) Georges, R.; Curely, J.; Drillon, J. *Appl. Phys.* **1985**, *58*, 914.

(30) Drillon, M.; Coronado, E.; Belaiche, M.; Carlin, R. L. *J. Appl. Phys.* **1988**, *63*, 3551.

(31) Drillon, M.; Belaiche, M.; Heintz, J. M.; Villeneuve, G.; Boukhari, A.; Aride, J. In *Organic and Inorganic Low-Dimensional Crystalline Materials*; Delhaes, P., Drillon, M., Eds.; NATO ASI Series 168; Plenum: New York, 1987; p 421.

Contribution from the Department of Chemistry, Gorlaeus Laboratories, Leiden University, P.O. Box 9502, 2300 RA Leiden, The Netherlands

Synthesis, Structure, and Properties of a Trinuclear and a Mononuclear Nickel(II) Complex of *N*,*N*′-Dimethyl-*N*,*N*′-bis(β-mercaptoethyl)ethylenediamine

Mary A. Turner, Willem L. Driessen, and Jan Reedijk*

Received January 24, 1990

The N_2S_2 ligand *N*,*N*′-dimethyl-*N*,*N*′-bis(β-mercaptoethyl)ethylenediamine, H_2L, reacts with $NiCl_2{\cdot}6H_2O$ in methanol solution to yield a trinuclear species of stoichiometry $[Ni_3L_2]Cl_2{\cdot}2H_2O$. This compound crystallizes in the monoclinic space group $P2_1/n$ with a = 19.917 (7) Å, b = 5.453 (3) Å, c = 13.508 (6) Å, β = 100.81 (4)°, and Z = 2. The trinuclear unit consists of two pseudosquare-planar terminal NiN_2S_2 environments arranged in a chair conformation about a central NiS_4 plane, with the central nickel occupying a crystallographic inversion center. A dihedral angle of 107.84 (7)° exists between nickel planes unrelated by symmetry. Ni–N distances are 1.938 (4) and 1.951 (3) Å, Ni–S distances in the NiN_2S_2 environment are 2.144 (1) and 2.160 (1) Å, and Ni–S distances of the NiS_4 center are 2.219 (1) and 2.216 (1) Å. The same ligand, under aprotic conditions, reacts with bis(acetylacetonato)nickel(II) to give a neutral mononuclear [NiL] unit with an NiN_2S_2 chromophore. The trinuclear and mononuclear species are compared with respect to their syntheses and NMR and electronic absorption spectra.

Introduction

The partial characterization of the nickel site in bacterial hydrogenases has prompted efforts to model the nickel environment in these proteins.[1-8] Features of the enzyme active site typically taken as modeling criteria are ligation of a Ni(III) center by anionic sulfur ligands—evidence for which has been observed in

(1) Kruger, H.-J.; Holm, R. H. *Inorg. Chem.* **1989**, *28*, 1148.

0020-1669/90/1329-3331$02.50/0